VIETNAM ACADEMY OF SCIENCE AND TECHNOLOGY

Vietnam Journal of MECHANICS

Volume 35 Number 2

ISSN 0866-7136

VN INDEX 12.666

2
2013

35th Anniversary

Vietnam Journal of Mechanics, VAST, Vol. 35, No. 2 (2013), pp. 131 – 145

MONITORING BREATHING CRACKS OF A BEAM-LIKE BRIDGE SUBJECTED TO MOVING VEHICLE USING WAVELET SPECTRUM

Nguyen Viet Khoa
Institute of Mechanics, Vietnam Academy of Science and Technology
18 Hoang Quoc Viet, Cau Giay, Hanoi
E-mail: nvkhoa@imech.ac.vn

Abstract. In this paper a wavelet spectrum technique for monitoring the breathing crack phenomenon of a beam-like bridge subjected to moving vehicle is presented. The stiffness of element with a breathing crack is modeled as a time dependent stiffness matrix using the finite element method. The stiffness matrix of the structure at each moment depends on the curvature of the structure at the crack position. The breathing crack phenomenon can be detected by analysing the instantaneous frequency (IF) of the system using the wavelet spectrum. When the crack depth is large, the crack area might be determined by the significant peak in the IF. The simulation results show that when the crack "breaths" the amplitude of the vibration obtained from the vehicle is smaller than in the case of an open crack. This is a warning when using the amplitude of the dynamic response to estimate the crack depth when there is a breathing crack in the structure. Therefore, it is important to distinguish the open crack and breathing crack to obtain a more accurate estimation of the crack depth. The results showed that crack with a depth as small as 10% of the beam height can be detected by the method. The proposed method can be applied with a noise level up to 10%.

Keywords: Breathing crack, crack detection, damage detection, moving vehicle, moving load, wavelet transform, wavelet-based method, wavelet spectrum.

1. INTRODUCTION

The monitoring of cracks in mechanical systems and civil engineering structures has attracted many researchers in the last two decades as reviewed by Salawu [1] and Doebling et al. [2]. There are many nondestructive methods for crack detection that are based on the changes in the dynamic properties of the structure (frequencies, mode shapes, transfer functions). Pandey and Biswas [3] presented a method for crack detection based on the difference between the flexibility matrices of the un-damaged and damaged structure. Verboven et al. [4, 5] presented autonomous damage detection methods based on modal parameters. In another study, Patjawit and Kanok-Nukulchai [6] proposed a method using Global Flexibility Index (GFI) for damage detection of highway bridges. This index is the spectral norm of the modal flexibility matrix obtained in association with selected reference points sensitive to the deformation of the bridge structure.

In the last two decade, the wavelet transform has been applied widely in many engineering fields since it can present a signal in both time and frequency domains. Wang and Deng [7] applied the Haar wavelet to investigate open cracked structures. Hong et al. [8] investigated the effectiveness of the continuous wavelet transform (CWT) in terms of its capability to estimate the Lipschitz exponent. Gentile and Messina [9] investigated mode shapes using CWT the position of the open crack in beam structures subjected to transverse vibration. A double-cracked beam was studied by Loutridis et al. [10]. The fundamental vibration mode of a double-cracked cantilever beam was analyzed using CWT. Recently, Castro et al. [11, 12] presented a wavelet based technique for detection of defects in rods subject to free and forced vibration.

In bridge engineering many applications have been found from this subject. Lin and Trethewey [13], presented a finite element analysis of elastic beams subjected to moving dynamic loads. Mahmoud and Abou Zaid [14] proposed an iterative modal analysis approach to determine the effect of transverse cracks on the dynamic behavior of simply supported undamped Bernoulli-Euler beams subject to a moving mass. Lee et al. [15] proposed a procedure consisting of identification of the operational modal properties and the assessment of damage locations and severities. Majumder and Manohar [16] presented a time domain formulation for damage detection of a beam using vibration response caused by a moving oscillator. Bilello and Bergman [17] studied damaged beams under a moving load. Zhu and Law [18] used continuous wavelet transform for analyzing the operational deflection time history of the bridge subject to a moving vehicular load. However, most of the current works relating to crack detection of a bridge subject to a moving vehicle focuses on fully open cracks, while the breathing crack phenomenon has not been concerned.

The aim of this study is to propose a wavelet spectrum technique for monitoring the breathing cracks of a beam-like bridge subjected to a moving vehicle. As the author's best knowledge, the work, using the combination of the wavelet spectrum and breathing crack phenomenon, for monitoring cracks of a vehicle-bridge system has not been investigated to date. The theoretical model of a beam-like bridge with breathing cracks and wavelet analysis are presented hereinafter. Numerical calculation is carried out to study the efficiency of the proposed technique.

2. DYNAMICS OF A BEAM-LIKE STRUCTURE UNDER MOVING VEHICLE

2.1. Intact beam like structure

Consider the bridge–vehicle system shown in Fig. 1. In this study the half-vehicle model is adopted from [19]. The bridge deck is modelled approximately as an Euler–Bernoulli beam. It is assumed that the surface unevenness of the bridge can be ignored and the tyres are always in contact with the supported beam. Under these assumptions the equation of motion for the bridge–vehicle system can be written as follows

$$\begin{bmatrix} I_0 & 0 & 0 & 0 \\ 0 & m_0 & 0 & 0 \\ 0 & 0 & m_1 & 0 \\ 0 & 0 & 0 & m_2 \end{bmatrix} \begin{Bmatrix} \ddot{d}_1 \\ \ddot{d}_2 \\ \ddot{d}_3 \\ \ddot{d}_4 \end{Bmatrix} + \begin{bmatrix} b_1^2 c_1 + b_2^2 c_2 & b_1 c_1 - b_2 c_2 & -b_1 c_1 & b_2 c_2 \\ b_1 c_1 - b_2 c_2 & c_1 + c_2 & -c_1 & -c_2 \\ -b_1 c & -c_1 & c_1 + c_3 & 0 \\ b_2 c_2 & -c_2 & 0 & c_2 + c_4 \end{bmatrix} \begin{Bmatrix} \dot{d}_1 \\ \dot{d}_2 \\ \dot{d}_3 \\ \dot{d}_4 \end{Bmatrix} +$$

$$+\begin{bmatrix} k_1b_1^2+k_2b_2^2 & k_1b_1-k_2b_2 & -k_1b_1 & k_2b_2 \\ k_1b_1-k_2b_2 & k_1+k_2 & -k_1 & -k_2 \\ -k_1b_1 & -k_1 & k_1+k_3 & 0 \\ k_2b_2 & -k_2 & 0 & k_2+k_4 \end{bmatrix} \begin{Bmatrix} d_1 \\ d_2 \\ d_3 \\ d_4 \end{Bmatrix} = \begin{Bmatrix} 0 \\ 0 \\ k_3u_1+c_3\dot{u}_1 \\ k_4u_2+c_4\dot{u}_2 \end{Bmatrix} \tag{1}$$

$$\mathbf{M}\ddot{\mathbf{d}}+\mathbf{N}\dot{\mathbf{d}}+\mathbf{C}\mathbf{d}=\mathbf{N}_1^T f_1+\mathbf{N}_2^T f_2 \tag{2}$$

where

$$f_1=-m_1g-m_1\ddot{d}_3-\frac{m_0gb_2}{b_1+b_2}-\frac{I_0\ddot{d}_1+m_0b_2\ddot{d}_2}{b_1+b_2}, \tag{3}$$

$$f_2=-m_2g-m_2\ddot{d}_4-\frac{m_0gb_1}{b_1+b_2}-\frac{I_0\ddot{d}_1+m_0b_1\ddot{d}_2}{b_1+b_2}, \tag{4}$$

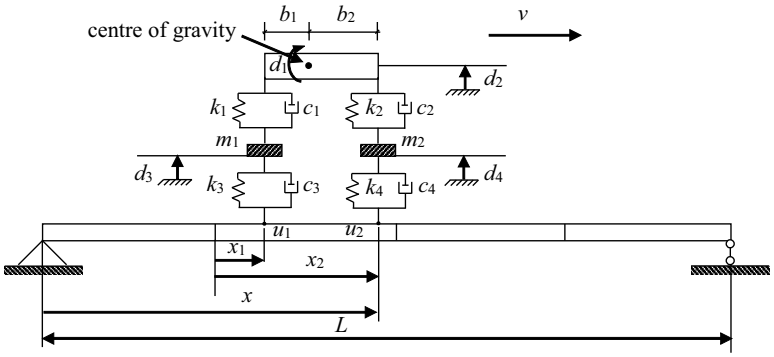

Fig. 1. A beam-like bridge under moving vehicle

where $I_0, b_1, b_2, m_0, m_1, m_2, k_1, k_2, k_3, k_4, c_1, c_2, c_3, c_4$ are vehicle parameters; d_1, d_2, d_3, d_4 are four vehicle degrees of freedom; v is the moving speed of vehicle; u_1, u_2 are the vertical displacements of the tyres and equal to the vertical displacement of the beam at the contact points 1 and 2. Structural parameters consist of: **M**, **C** and **K** - structural mass, damping and stiffness matrices. The interaction forces acting on the beam at contact points denoted by f_1 and f_2; g is gravitational acceleration; $\mathbf{N}^T$ is the transposition of the shape functions at the position x of the interaction force; **d** is the nodal displacement of the beam. From the nodal displacement **d** and the shape functions **N,** the displacement of the beam u at the arbitrary position x can be interpolated as [13]

$$\mathbf{u}=\mathbf{N}\mathbf{d} \tag{5}$$

The shape function of an element is defined as

$$\mathbf{N}=[N_1 \;\; N_2 \;\; N_3 \;\; N_4] \tag{6}$$

where

$$\begin{aligned} &N_1=1-3\left(\frac{x}{l}\right)^2+2\left(\frac{x}{l}\right)^3 \;\; ; \;\; N_2=x\left(\frac{x}{l}-1\right)^2 \;\; ; \\ &N_3=3\left(\frac{x}{l}\right)^2-2\left(\frac{x}{l}\right)^3 \;\; ; \;\; N_4=x\left[\left(\frac{x}{l}\right)^2-\frac{x}{l}\right] \end{aligned} \tag{7}$$

with l being the length of the element. The time derivatives of u are

$$\dot{u}(x,t) = \frac{\partial u}{\partial x}\dot{x} + \frac{\partial u}{\partial t} \tag{8}$$

Because $\mathbf{N}$ is a spatial function while $\mathbf{d}$ is time dependent, from (5) we have

$$\frac{\partial u}{\partial x} = \mathbf{N_x d} \tag{9}$$

where the subscript x implies the differentiation with respect to x. Substituting (8) and (9) into Eqs. (1) and (2) yields

$$\begin{pmatrix} \mathbf{M} & \sum_{i=1}^{2}\mathbf{N}_i^T f_{\theta i} & \sum_{i=1}^{2}\mathbf{N}_i^T f_{yi} & m_1\mathbf{N}_1^T & m_2\mathbf{N}_2^T \\ \mathbf{O} & I_0 & 0 & 0 & 0 \\ \mathbf{O} & 0 & m_0 & 0 & 0 \\ \mathbf{O} & 0 & 0 & m_1 & 0 \\ \mathbf{O} & 0 & 0 & 0 & m_2 \end{pmatrix} \begin{pmatrix} \ddot{\mathbf{d}} \\ \ddot{d}_1 \\ \ddot{d}_2 \\ \ddot{d}_3 \\ \ddot{d}_4 \end{pmatrix}$$

$$+ \begin{pmatrix} \mathbf{C} & \mathbf{O}^T & \mathbf{O}^T & \mathbf{O}^T & \mathbf{O}^T \\ \mathbf{O} & b_1^2c_1 + b_2^2c_2 & b_1c_1 - b_2c_2 & -b_1c_1 & b_2c_2 \\ \mathbf{O} & b_1c_1 - b_2c_2 & c_1 + c_2 & -c_1 & -c_2 \\ -c_3\mathbf{N}_1 & -b_1c_1 & -c_1 & c_1 + c_3 & 0 \\ -c_4\mathbf{N}_2 & b_2c_2 & -c_2 & 0 & c_2 + c_4 \end{pmatrix} \begin{pmatrix} \dot{\mathbf{d}} \\ \dot{d}_1 \\ \dot{d}_2 \\ \dot{d}_3 \\ \dot{d}_4 \end{pmatrix}$$

$$+ \begin{pmatrix} \mathbf{K} & \mathbf{O}^T & \mathbf{O}^T & \mathbf{O}^T & \mathbf{O}^T \\ \mathbf{O} & k_1b_1^2 + k_2b_2^2 & k_1b_1 - k_2b_2 & -k_1b_1 & -k_2b_2 \\ \mathbf{O} & k_1b_1 - k_2b_2 & k_1 + k_2 & -k_1 & -k_2 \\ -k_3\mathbf{N}_1 - c_3\mathbf{N}_{1x}\dot{x}_1 & -k_1b_1 & -k_1 & k_1 + k_3 & 0 \\ -k_4\mathbf{N}_2 - c_4\mathbf{N}_{2x}\dot{x}_2 & -k_2b_2 & -k_2 & 0 & k_2 + k_4 \end{pmatrix} \begin{pmatrix} \mathbf{d} \\ d_1 \\ d_2 \\ d_3 \\ d_4 \end{pmatrix} = \begin{pmatrix} \sum_{i=1}^{2}\mathbf{N}_i^T \hat{f}_i \\ 0 \\ 0 \\ 0 \\ 0 \end{pmatrix} \tag{10}$$

where $\mathbf{O}$ is a zero row matrix, and

$$f_{\theta 1} = \frac{1}{b_1 + b_2}I_0, f_{\theta 2} = -\frac{1}{b_1 + b_2}I_0, f_{y1} = \frac{b_2}{b_1 + b_2}m_0, f_{y2} = \frac{b_1}{b_1 + b_2}m_0, \tag{11}$$

$$\hat{f}_1 = -\frac{b_2}{b_1 + b_2}m_0 g - m_1 g \quad , \quad \hat{f}_2 = -\frac{b_1}{b_1 + b_2}m_0 g - m_2 g \tag{12}$$

2.2. Multi-cracked beam like structure

2.2.1. *Stiffness matrix of an open cracked element*

Fig. 2 shows a uniform beam-like structure divided into Q elements with R cracks located in R different elements. A brief description for deriving the element stiffness matrix of an open cracked element is presented here, while more details can be obtained from previous works [13]. Neglecting shear action, the strain energy of an element without a crack can be written as

$$W^{(0)} = \frac{1}{2EI}\left(M^2 l + MPl^2 + \frac{P^2 l^3}{3}\right) \tag{13}$$

where P and M are the shear and bending internal forces at the right node of the element. The additional energy due to the crack of a rectangular beam with thickness h and width b can be expressed as follows

$$W^{(1)} = b \int_0^a \left(\frac{\left(K_I^2 + K_{II}^2\right)}{E'} + \frac{(1+\nu) K_{III}^2}{E} \right) da \tag{14}$$

where $E' = E$ for plane stress, $E' = \dfrac{E}{1-\nu^2}$ for plane strain and a is the crack depth, and K_I, K_{II}, K_{III} are stress intensity factors for opening type, sliding type and tearing type cracks, respectively. Taking into account only bending, Eq. (14) leads to

$$W^{(1)} = b \int_0^a \frac{(K_{IM} + K_{IP})^2 + K_{IIP}^2}{E'} da \tag{15}$$

where

$$K_{IM} = \frac{6M\sqrt{\pi a} F_I(s)}{bh^2}\,;\; K_{IP} = \frac{3Pl\sqrt{\pi a} F_I(s)}{bh^2}\;;\; K_{IIP} = \frac{P\sqrt{\pi a} F_{II}(s)}{bh} \tag{16}$$

$$F_I(s) = \sqrt{\frac{2}{\pi s} tg\left(\frac{\pi s}{2}\right)} \frac{0.923 + 0.199\left[1 - \sin\left(\dfrac{\pi s}{2}\right)\right]^4}{\cos\left(\dfrac{\pi s}{2}\right)} \tag{17}$$

$$F_{II}(s) = \left(3s - 2s^2\right) \frac{1.122 - 0.561s + 0.085s^2 + 0.18s^3}{\sqrt{1-s}} \tag{18}$$

Components of the flexibility matrix $\tilde{\mathbf{C}}$ of the intact element can be calculated as

$$\tilde{c}_{ij}^{(0)} = \frac{\partial^2 W^{(0)}}{\partial P_i \partial P_j}\,;\quad i,j = 1,2\;;\;\; P_1 = P\,;\;\; P_2 = M \tag{19}$$

The additional flexibility coefficient is

$$\tilde{c}_{ij}^{(1)} = \frac{\partial^2 W^{(1)}}{\partial P_i \partial P_j}\,;\quad i,j = 1,2\;;\;\; P_1 = P\,;\;\; P_2 = M \tag{20}$$

The total flexibility coefficient is then the sum of the flexibility coefficient of the intact element and the additional flexibility coefficient due to the crack

$$\tilde{c}_{ij} = \tilde{c}_{ij}^{(0)} + \tilde{c}_{ij}^{(1)} \tag{21}$$

From the equilibrium condition the following equation can be obtained

$$\begin{pmatrix} P_i & M_i & P_{i+1} & M_{i+1} \end{pmatrix}^T = \mathbf{T} \begin{pmatrix} P_{i+1} & M_{i+1} \end{pmatrix}^T \tag{22}$$

where

$$\mathbf{T} = \begin{pmatrix} -1 & -L & 1 & 0 \\ 0 & -1 & 0 & 1 \end{pmatrix}^T \tag{23}$$

The stiffness matrix of the cracked element is derived by applying the principle of virtual work

$$\mathbf{K_c} = \mathbf{T}^T \tilde{\mathbf{C}} \mathbf{T} \tag{24}$$

2.2.2. *Stiffness matrix of a breathing cracked element*

When a breathing crack is present in the bridge, there is experimental evidence that the crack opens and closes gradually leading to a gradual change in the stiffness at the cross section of the crack during vibration. To model the breathing crack the stiffness of a cracked element can be determined using the curvature of the beam at the crack location [20]. It is assumed that the effect of crack depends on the curvature of beam at crack location and it ranges from 0 to 1 when the curvature ranges from negative maximum to positive maximum. As a result, the stiffness matrix $\mathbf{K}$ of the breathing cracked element can be modelled as follows

$$\mathbf{K_b} = \mathbf{K_e} + \frac{1}{2}(\mathbf{K_c} - \mathbf{K_e}) \left[1 + \frac{d''}{d''_{\max}}\right] \tag{25}$$

Where, $\mathbf{K_b}$ and $\mathbf{K_c}$ are the stiffness of the element with breathing crack, open crack and $\mathbf{K_e}$ is the stiffness of the intact element. d'' is the instantaneous curvature of the beam at the crack position and $d''_{\max}$ is the maximum curvature of the beam at the crack position during motion of the vehicle. Eq. (25) shows that when $d'' = -d''_{\max}$ the stiffness $\mathbf{K_b}$ is minimum and equal to $\mathbf{K_e}$ – the stiffness of an intact element. When $d'' = d''_{\max}$ the stiffness $\mathbf{K_b}$ is maximum and equal to $\mathbf{K_c}$ – the stiffness of an open cracked element. By this method, the stiffness of a breathing cracked element can be determined based on the stiffness of an open cracked and intact element without reference to a known frequency. Therefore, in this work Eq. (25) will be used to calculate the stiffness matrix of the breathing cracked beam.

2.2.3. *Global matrices of a beam like structure*

The stiffness matrix and mass matrix for an element without a crack are obtained from finite element model

$$\mathbf{K_e} = \frac{EI}{l^3} \begin{bmatrix} 12 & 6l & -12 & 6l \\ 6l & 4l^2 & -6l & 2l^2 \\ -12 & -6l & 12 & -6l \\ 6l & 2l^2 & -6l & 4l^2 \end{bmatrix} \tag{26}$$

$$\mathbf{M_e} = \frac{ml}{420} \begin{bmatrix} 156 & 22l & 54 & -13l \\ 22l & 4l^2 & 13l & -3l^2 \\ 54 & 13l & 156 & -22l \\ -13l & -3l^2 & -22l & 4l^2 \end{bmatrix} \tag{27}$$

where I is the moment of inertia; E is the Young's modulus and m and l are the mass and the length of the element respectively.

The global mass matrix $\mathbf{M}$ is assembled from element mass matrices $\mathbf{M_e}$ and global stiffness matrix $\mathbf{K}$ of the breathing cracked beam is assembled from element stiffness $\mathbf{K_e}$ and $\mathbf{K_b}$. Rayleigh damping in the form of $\mathbf{C} = \alpha\mathbf{M} + \beta\mathbf{K}$ adopted from [13] is used for the beam.

Solving Eq. (10) with the global matrices $\mathbf{M}$, $\mathbf{C}$, and $\mathbf{K}$ of the breathing cracked beam, the dynamic responses of the vehicle and the beam will be obtained.

3. WAVELET SPECTRUM

The continuous wavelet transform is defined as follows [21]

$$W(a,b) = \int_{-\infty}^{+\infty} f(t)\psi_{a,b}dt \tag{28}$$

Where $\psi_{a,b}(t) = \frac{1}{\sqrt{a}}\psi^*\left(\frac{t-b}{a}\right)$, a is a real number called scale or dilation, b is a real number called position, $W(a,b)$ are wavelet coefficients at scale a and position b, $f(t)$ is input signal, $\psi\left(\frac{t-b}{a}\right)$ is wavelet function and $\psi^*\left(\frac{t-b}{a}\right)$ is complex conjugate of $\psi\left(\frac{t-b}{a}\right)$. In order to be classified as a wavelet a function must satisfy the following mathematical criteria

1) A wavelet must have finite energy

$$E = \int_{-\infty}^{+\infty} |\psi(t)|^2 dt < \infty \tag{29}$$

2) If $\hat{\psi}(\omega)$ is Fourier transform of $\psi(t)$, i.e.

$$\hat{\psi}(\omega) = \int_{-\infty}^{+\infty} \psi(t) e^{-i\omega t} dt \tag{30}$$

then the following condition must be satisfied

$$C_g = \int_0^{\infty} \frac{\left|\hat{\psi}(\omega)\right|^2}{\omega} d\omega < \infty \tag{31}$$

This implies that the wavelet has no zero frequency component: $\hat{\psi}(0) = 0$,

$$\int_{-\infty}^{+\infty} \psi(t) e^{-j\omega t} dt = 0 \quad \text{when } \omega = 0 \tag{32}$$

or in other words, the wavelet must have a zero mean

$$\int_{-\infty}^{+\infty} \psi(t) dt = 0 \tag{33}$$

3) An additional criterion is that, for complex wavelets, the Fourier transform must both be real and vanish for negative frequencies.

The wavelet power spectrum is then simply defined as the square modulus of wavelet transform

$$S(a,b) = |W(a,b)|^2 \tag{34}$$

The stiffness of the beam with a breathing crack varies during vibration leading to the variation in the frequency of the beam. This variation of frequency cannot be detected by visually inspecting the vibration signal in the time domain or in the frequency domain. However, since the wavelet spectrum transforms the signal into the frequency domain while the time information is still retained, the wavelet spectrum as defined in (34) can be used to detect the variation of frequency during vibration. The square of the modulus of the wavelet transform or wavelet spectrum can be interpreted as an energy density distribution over the (a, b) time-scale plane. The energy of a signal is mainly concentrated on the time-scale plane around the ridges of the wavelet spectrum. Since the scale corresponds to the frequency of vibration, ridges of the time-scale plane correspond to the main frequencies of the signal. Thus, the IF of the signal can be observed by monitoring the ridges of the time-scale plane. For the purpose of convenience, the time-scale is converted to the time-frequency plane by relating the scale to the pseudo-frequency as follows

$$F_a = \frac{F_c}{a\Delta} \tag{35}$$

where a is a scale, Δ is the sampling period, F_c is the center frequency of a wavelet function in Hz, F_a is the pseudo-frequency corresponding to the scale a, in Hz.

Therefore, in order to monitor the IF of the vehicle-bridge system during vibration, the wavelet power spectrum $S(a, b)$, which provides a measure of the time series variance at each time and each scale is used in this study. Using the wavelet power spectrum to track the frequency of the vibration with main energy in time, the variation of the frequency during vibration or the IF will be determined.

4. SIMULATION RESULTS AND DISCUSSIONS

A numerical example of the beam with two cracks at locations of $Lc = L/3$ is carried out. Parameters of the beam are: mass density is 7855 kg/m^3; modulus of elasticity $E = 2.1 \times 10^{11}$ N/m^2; $L = 50$ m; $b = 0.5$ m; $h = 1$ m. Vehicle parameters are adopted from [22] as follows: $m_1 = m_2 = 50000$ N; $k = 1.0 \times 10^6$ N/m; $c = 5.0 \times 10^2$ Ns/m. For the crack detection problem, low vehicle speeds can be applied better than high speeds [18], thus the vehicle speed $v = 2$ m/s is used in this study. The displacement-time history of the moving vehicle is obtained to investigate the influence of the cracks.

4.1. Influences of breathing cracks on dynamic responses

Figs. 2-5 show the dynamic displacements of the vehicle moving on the bridge without a crack, with a fully open crack, and with a breathing crack calculated from four different levels of the cracks. As can be seen from these figures, the amplitude of the vertical displacement of vehicle moving on the bridge with the breathing crack is smaller than that with the open crack. However, the amplitude of the vertical displacement in the case of breathing crack is larger than the case of intact beam. This means that it is more difficult when using the amplitude of dynamic displacement to detect the crack if it behaves as a breathing crack. When the crack depth is large as can be seen in Fig. 3, the effect of the breathing crack can roughly be considered as the effect of a fully open crack with much smaller depth. This result is in agreement with the work in [20]. However, this

conclusion is not correct when the crack depth is small which was not discussed in [20]. As is seen in Fig. 2 when the crack depth is smaller than or equal to 30% of the beam height, the dynamic response in the case of a beam with a breathing crack is closer to the case of a beam with an open crack than the case of an intact beam. It is concluded that the amplitude of the response when the crack breaths is always smaller than the case of an open crack, especially when the crack depth is large the difference between them is very significant. Thus, in order to estimate the crack using the amplitude of the dynamic response, careful attention should be paid if there is an existence of the breathing crack phenomenon: the small amplitude of the response does not correspond to the small size of crack.

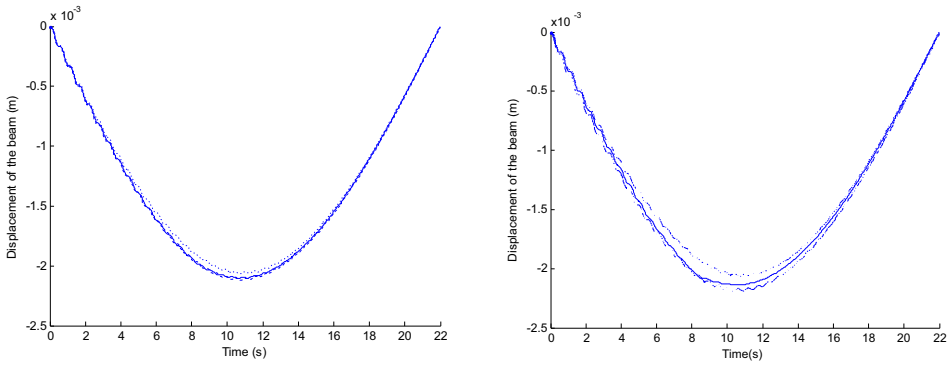

(a) Crack depth is 20% (b) Crack depth is 30%

Fig. 2. Vertical displacement of the vehicle
····· intact beam; ——— breathing crack; — · · — ·· open crack

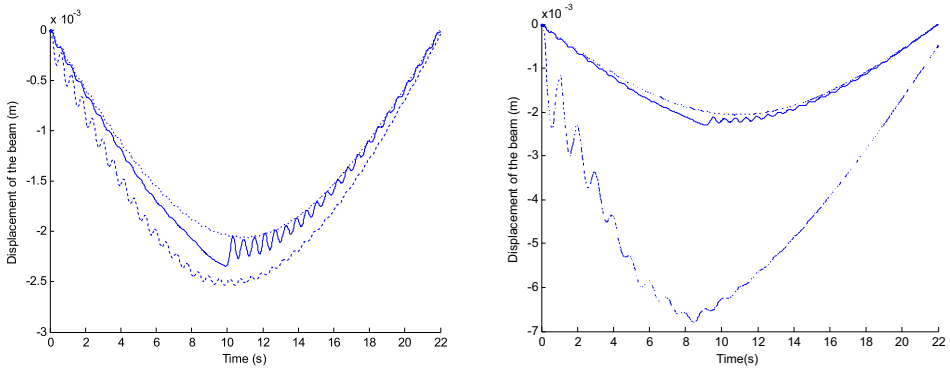

(a) Crack depth is 50% (b) Crack depth is 80%

Fig. 3. Vertical displacement of the vehicle
····· intact beam; ——— breathing crack; — · · — ·· open crack

4.2. Detection of breathing crack using instantaneous frequency

In order to detect the breathing crack phenomenon from the time-frequency plane, the ridge in the case of a breathing cracked beam is compared with the ridge in the case of an open cracked beam. Figs. 4-5 present the time-frequency plane of the wavelet spectrum of the vertical displacement signal for the case of an open crack and a breathing crack. As can be seen in Fig. 4 for the case of open crack the energy of the signal is mainly concentrated on the frequency of approximately 1.6 Hz. However, in the case of a breathing crack, as can be seen in Fig. 5, the main frequency is varied, not a constant. Therefore, ridges in the time-frequency plane can be used to detect the breathing crack phenomenon. For this purpose, the main ridge of time-frequency plane is extracted from the time-frequency plane as in Figs. 6-10 for five crack levels ranging from 10% to 50%.

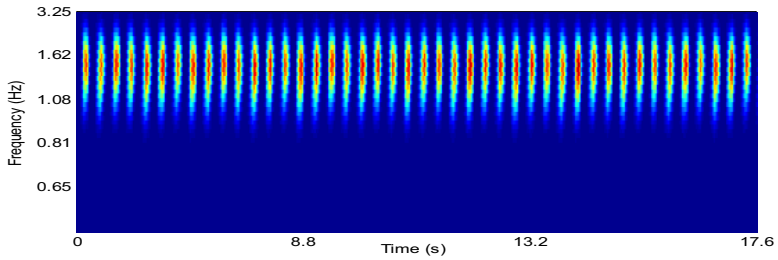

Fig. 4. Wavelet spectrum of the vertical displacement of the vehicle, crack depth is 50%: Open crack

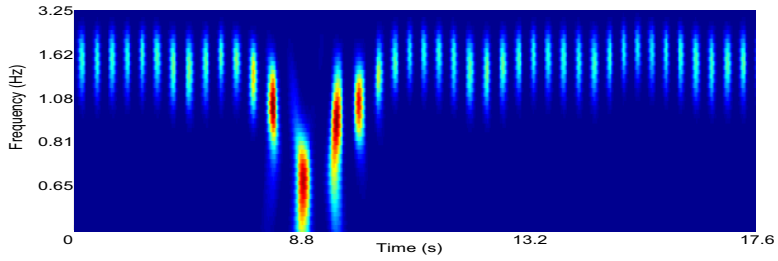

Fig. 5. Wavelet spectrum of the vertical displacement of the vehicle, crack depth is 50%: Breathing crack

As can be seen in Figs. 6-10 when the crack is open (graphs a), the IFs are approximately constant during vibration due to the constant stiffness. However, in case of breathing crack (graphs b), the IFs are varied since the stiffness of the beam varies during vibration. This means that the variation of the IF in the time-frequency plane indicates the breathing crack phenomenon, while the constant IF means the crack is open. When the crack depth is small the amplitude of the variation of the ridge is small and when the crack depth increases, this amplitude increases. Especially, when the crack depth is larger than or equal to 30% the IF has a significant change at the time around $t = 8.3$ s corresponding to the moment the vehicle passes by the crack. The reason is that, when

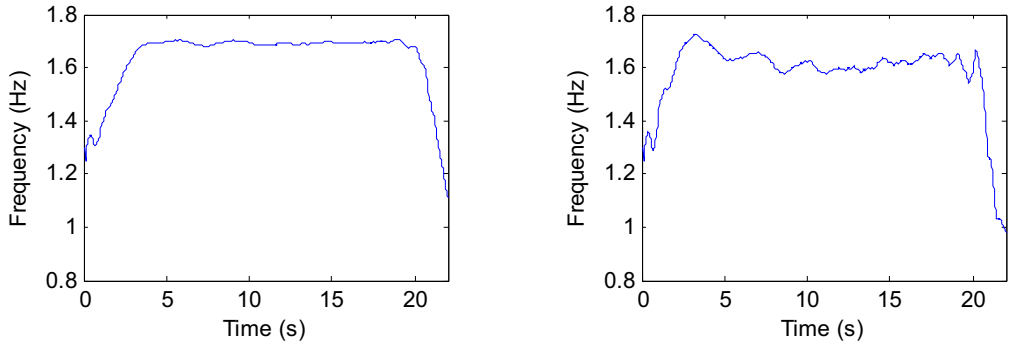

(a) Open crack (b) Breathing crack

Fig. 6. Wavelet ridge, crack depth is 10%

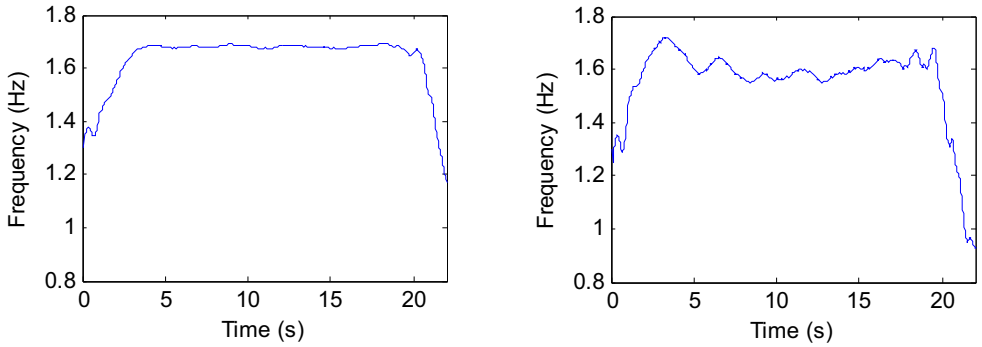

(a) Open crack (b) Breathing crack

Fig. 7. Wavelet ridge, crack depth is 20%

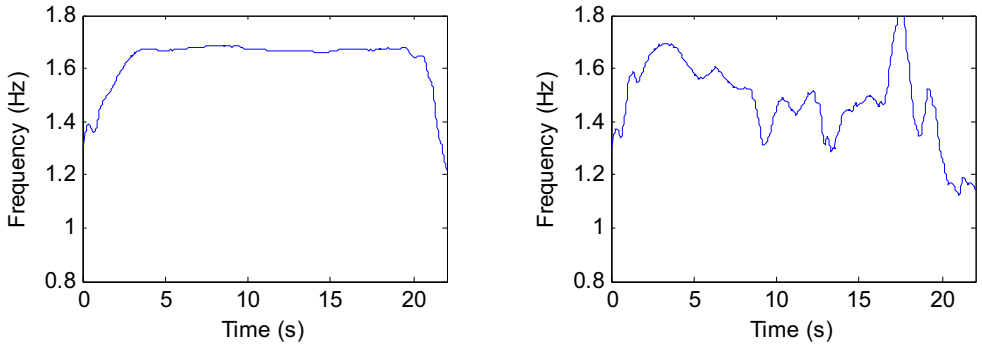

(a) Open crack (b) Breathing crack

Fig. 8. Wavelet ridge, crack depth is 30%

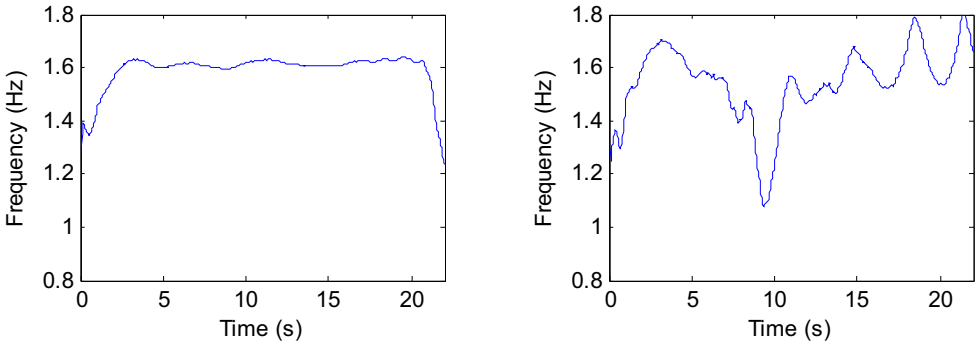

(a) Open crack (b) Breathing crack

Fig. 9. Wavelet ridge, crack depth is 40%

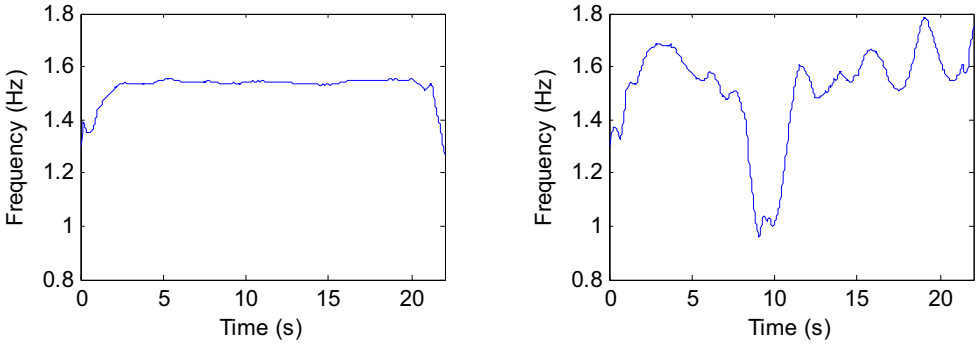

(a) Open crack (b) Breathing crack

Fig. 10. Wavelet ridge, crack depth is 50%

the vehicle passes by the crack location it will open significantly the crack causing the stiffness at the crack location smallest and in turn it leads to a significant change in the IF. Thus, in such cases, the significant peak in the IF can be used to determine the crack area.

Note that the continuous wavelet transform has an edge effect then there are distortions at the beginning and end of the wavelet ridge in Figs. 6-10 (for example at 2 s and 20 s). Thus, the values at the beginning and end of the IF in these figures are not real and can be disregarded.

4.3. Influence of the noise

In order to simulate the polluted measurements, white noise is added to calculated responses of the vehicle. The noisy response is calculated as follows [20]

$$d_{2noisy} = d_2 + E_p N \sigma(d_2) \tag{36}$$

where d_2 is the vertical displacement of the vehicle body obtained from the numerical simulation. E_p is the noise level and N is a standard normal distribution vector with zero

mean value and unit standard deviation. d_{2noisy} is the noisy displacement, and $\sigma(d_2)$ is its standard deviation.

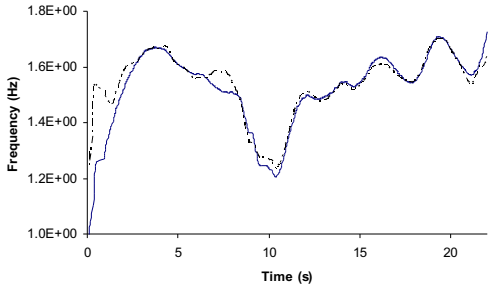

Fig. 11. Wavelet ridge, breathing crack, crack depth is 50%, $v = 2$ m/s. Solid line: 0 % noise; dotted line: 10 % noise

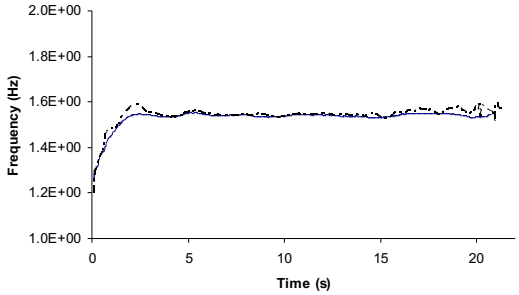

Fig. 12. Wavelet ridge, open crack, crack depth is 50%, $v = 2$ m/s. Solid line: 0 % noise; dotted line: 10 % noise

Fig. 11 shows the graphs of IF versus time of the breathing cracked beam with a crack depth of 50%. As can be seen from this figure, the IFs in the two cases, noisy and unnoisy, vary with time illustrating the phenomenon of the breathing cracks. The influence of the noise on the IF in the case of an open crack is also investigated. Fig. 12 presents two IFs of the two cases, noisy and unnoisy, versus time in case of an open crack with the crack depth of 50%. As can be seen from this figure, the two IFs are very close together and remain almost constant with time. This means that a noise level up to 10% does not particularly influence the IFs in both cases of open and breathing cracks. Thus, the graph of IF versus time can be used to detect the breathing crack phenomenon with a noise level up to 10%. Meanwhile, the method can only be applied with a noise level of 5% in the case of open cracks [20]. This means that when there is a presence of the breathing crack, the proposed method works more efficiently in a noisy environment when compared with the case of open crack.

5. CONCLUSION

In this paper, a wavelet spectrum technique for detection of breathing cracks of a vehicle-bridge system using the dynamic response of the vehicle-bridge is presented. A warning for crack detection of the system with the presence of a breathing crack is suggested.

The amplitude of the response of the vehicle moving on a beam-like bridge with breathing cracks is always smaller than that of open cracks. Especially, when the crack depth large, the difference in responses in the case of breathing cracks and in the case of fully open cracks is very large larger. Therefore, careful inspection needs to be carried out when using the amplitude of response to assess the crack size: the small measured amplitude of response does not always correspond to a small crack size as reported for the case of open crack it is in fact larger if there is the existence of a breathing crack. Thus,

it is important to distinguish the open and breathing cracks in order to have an accurate assessment of the crack depth.

Breathing cracks can be detected by the variation of the IF in the wavelet spectrum during vibration. When the crack depth increases, the variation of the IF increases. When the crack depth is large, the position of the largest peak in the IF might be used to determine the crack area.

The method can be applied for the case of polluted measurements with a noise level up to 10% when there is a presence of breathing cracks, while it is only 5% if the cracks are fully open during vibration. Therefore, the proposed method is more efficient with the presence of breathing cracks in comparison with the case of fully open cracks.

ACKNOWLEDGEMENT

This work is supported by National Foundation for Science and Technology Development (NAFOSTED) 2012-2013.

REFERENCES

[1] Salawu O.S., Detection of structural damage through changes in frequency: a review, *Engineering Structures*, **19**(9), (1997), pp. 718–723.

[2] Doebling S.W., Farrar C.R., Prime M.B., A summary review of vibration-based damage identification methods, *The Shock and Vibration Digest*, **30**(2), (1998), pp. 91–105.

[3] Pandey A. K. and Biswas M., Damage detection in structures using changes in flexibility, *Journal of Sound and Vibration*, **169**(1), (1994), pp. 3-17.

[4] Verboven P., Parloo E., Guillaume P. and Overmeire M. V., Autonomous structural health monitoring - Part I: Modal parameter estimation and tracking, *Mechanical Systems and Signal Processing*, **16**(4), (2002), pp. 637-657.

[5] Verboven P., Parloo E., Guillaume P. and Overmeire M. V., Autonomous structural health monitoring - Part II: Vibration-based in-operation damage assessement, *Mechanical Systems and Signal Processing*, **16**(4), (2002), pp. 659-675.

[6] Patjawit A, Kanok-Nukulchai W., Health monitoring of highway bridge based on a global flexibility index, *Engineering Structures*, **27**, (2005), pp. 1385-1391.

[7] Wang Q. and Deng X., Damage detection with spatial wavelets, *International Journal of Solids and Structures*, **36**, (1999), pp. 3443-3468.

[8] Hong J.-C., Kim Y.Y., Lee H.C., and Lee Y.W., Damage detection using the lipschitz exponent estimated by the wavelet transform: Applications to vibration modes of a beam, *International Journal of Solids and Structures*, **39**, (2002), pp. 1803-1816.

[9] Gentile A. and Messina A., On the continuous wavelet transforms applied to discrete vibration data for detecting open cracks in damaged beams, *International Journal of Solids and Structures*, **40**, (2003), pp. 295-315.

[10] Loutridis S., Douka E., and Trochidis A., Crack identification in double-cracked beam using wavelet analysis, *Journal of Sound and Vibration*, **277**, (2004), pp. 1025–1039.

[11] Castro E., Garcia-Hernandez M. T., Gallego A., Damage detection in rods by means of the wavelet analysis of vibration: Influence of the mode order, *Journal of Sound and Vibration*, **296**, (2006), pp. 1028-1038.

[12] Castro E., Garcia-Hernandez M. T., Gallego A., Defect identification in rods subject to forced vibration using the spatial wavelet transform, *Journal of Sound and Vibration*, accepted 13 April 2006.
[13] Lin Y. H. and Trethewey M. W., Finite element analysis of elastic beams subjected to moving dynamic loads, *Journal of Sound and Vibration*, **136**(2), (1989), pp. 323-342.
[14] Mahmoud M. A. and Abouzaid M. A., Dynamic response of a beam with a crack subject to a moving mass, *Journal of Sound and Vibration*, **256**(4), (2002), pp. 591-603.
[15] Lee J.W., Kim J.D., Yun C.B., Yi J.H., Shim J.M., Health-monitoring method for bridges under ordinary traffic loadings, *Journal of Sound and Vibration*, **257**(2), (2002), pp. 247–264.
[16] Majumder L. and Manohar C.S., A time-domain approachfor damage detection in beam structures using vibration data witha moving oscillator as an excitation source, *Journal of Sound and Vibration*, **268**, (2002), pp. 699–716.
[17] Bilello C., Bergman L.A., Vibration of damaged beams under a moving mass: Theory and experimental validation, *Journal of Sound and Vibration*, **274**, pp. 567–582.
[18] Zhu X.Q., Law S.S., Wavelet-based crack identification of bridge beam from operational deflection time history, *International Journal of Solids and Structures*, (2006), **43**, pp. 2299–2317.
[19] Jazar R.N., *Vehicle dynamics theory and application*, Springer, New York, (2008).
[20] Ariaei A., Ziaei-Rad S. and Ghayour M., Vibration analysis of beams with open and breathing cracks subjected to moving masses, *Journal of Sound and Vibration*, **326**, (2009), pp. 709-724.
[21] Daubechies I., *Ten lectures on wavelets*, CBMS-NSF Conference series, 61. Philadelphia, PA: SISAM, (1992).
[22] L. Deng, C.S. Cai, Identification of parameters of vehicles moving on bridges, *Engineering Structures*, **31**, (2009), pp. 2474–2485.

Received February 02, 2013

VIETNAM ACADEMY OF SCIENCE AND TECHNOLOGY
VIETNAM JOURNAL OF MECHANICS VOLUME 35, N. 2, 2013

CONTENTS